PNAS RESEARCH ARTICLE | PHYSICS OPEN ACCESS

Large phonon thermal Hall conductivity in the antiferromagnetic insulator Cu_3TeO_6

Lu Chen[a,1], Marie-Eve Boulanger[a,1], Zhi-Cheng Wang[b], Fazel Tafti[b], and Louis Taillefer[a,c,2]

Edited by J. C. Davis, University of Oxford, United Kingdom; received May 16, 2022; accepted July 18, 2022

Phonons are known to generate a thermal Hall effect in certain insulators, including oxides with rare-earth impurities, quantum paraelectrics, multiferroic materials, and cuprate Mott insulators. In each case, a special feature of the material is presumed relevant for the underlying mechanism that confers chirality to phonons in a magnetic field. A fundamental question is whether a phonon Hall effect is an unusual occurrence—linked to special characteristics such as skew scattering off rare-earth impurities, structural domains, ferroelectricity, or ferromagnetism—or a much more common property of insulators than hitherto believed. To help answer this question, we have turned to a material with none of the previously encountered special features: the cubic antiferromagnet Cu_3TeO_6. We find that its thermal Hall conductivity κ_{xy} is among the largest of any insulator so far. We show that this record-high κ_{xy} signal is due to phonons, and it does not require the presence of magnetic order, as it persists above the ordering temperature. We conclude that the phonon Hall effect is likely to be a fairly common property of solids.

thermal Hall effect | antiferromagnetism | phonons | impurities | thermal conductivity

Significance

Phonons are believed not to be able to generate a thermal Hall signal due to their lack of charge or spin. However, since the first discovery of a phonon thermal Hall effect in the paramagnetic insulator $Tb_3Ga_5O_{12}$, much larger signals have been observed in several other families of insulators, which raises a fundamental question: How can phonons become chiral in a magnetic field? Most of the insulators that exhibit a phonon Hall effect have some special feature, believed to be a key to the underlying mechanism. Here, our discovery of a large phonon thermal Hall conductivity in a simple material with none of the special features of the previous cases opens up the subject into a much broader question.

The thermal Hall effect is the thermal analog of the electrical Hall effect. Instead of a transverse voltage induced by a perpendicular magnetic field in the presence of an electric current, a transverse temperature difference is induced in the presence of a heat current. The thermal Hall effect is a consequence of what we call "chirality"—which we define as a handedness that heat carriers acquire in a magnetic field. Electrons acquire chirality through the Lorentz force acting on charge carriers. However, understanding how chirality arises for electrically neutral particles—like phonons, magnons, or more exotic excitations—relies on new and mostly unknown mechanisms.

The phonon thermal Hall effect was first observed in the insulator $Tb_3Ga_5O_{12}$ (1, 2), whose small thermal Hall conductivity κ_{xy} was attributed to a special skew scattering of phonons by superstoichiometric Tb impurities (3). Later on, a much larger κ_{xy} was measured in the multiferroic material $Fe_2Mo_3O_8$, a ferrimagnetic insulator, where it was attributed to phonons in the presence of strong spin-lattice coupling (4). More recently, an even larger κ_{xy} was reported in two other families of insulators: the cuprate Mott insulators (5–8), such as La_2CuO_4 and $Sr_2CuO_2Cl_2$, and the quantum paraelectric $SrTiO_3$ (9). There is little doubt that phonons are the bearers of chirality in both families, but the underlying mechanisms for the thermal Hall effect remain unknown.

The origin of phonon chirality is an open question. There are two classes of scenarios: scenarios based on the coupling of phonons to their pristine environment and scenarios based on the scattering of phonons by impurities or defects. For $SrTiO_3$, the first type of scenario includes the flexoelectric coupling of phonons to their nearly ferroelectric environment, and the second type of scenario includes the scattering of phonons from structural domains (10). For cuprates, the first type includes the coupling of phonons to magnons (11) or spinons (12, 13), a special magnetoelectric order parameter (14), or an intrinsic fluctuating field arising from spin–lattice coupling (15). The second type includes the scattering of phonons by oxygen vacancies (16), by pointlike impurities in the presence of a Hall viscosity due to a coupling of phonons to their electronic environment (17), and by impurities and defects through the resonant skew-scattering process (18) or the "side-jump" effect (19).

In this article, we provide insights on the origin of phonon chirality by turning to a completely different and simpler material: Cu_3TeO_6. This is an insulator with a cubic structure, which retains its structure down to low temperature and therefore does not harbor structural domains. It also does not contain rare-earth elements and is neither a Mott insulator nor a multiferroic or nearly ferroelectric material. It develops three-dimensional long-range collinear antiferromagnetic order below the Néel temperature $T_N = 63$ K (20, 21).

Author affiliations: [a]Département de Physique, Institut Quantique and Regroupement Québécois sur les Matériaux de Pointe, Université de Sherbrooke, Sherbrooke, QC J1K 2R1, Canada; [b]Department of Physics, Boston College, Chestnut Hill, MA 02467; and [c]Canadian Institute for Advanced Research, Toronto, ON M5G 1M1, Canada

Author contributions: L.C., M.-E.B., and L.T. designed research; L.C. and M.-E.B. performed research; L.C. and M.-E.B. analyzed data; L.C., M.-E.B., Z.-C.W., F.T., and L.T. wrote the paper; and Z.-C.W. and F.T. provided the samples.

The authors declare no competing interest.

This article is a PNAS Direct Submission.

Copyright © 2022 the Author(s). Published by PNAS. This open access article is distributed under Creative Commons Attribution License 4.0 (CC BY).

[1]L.C. and M.-E.B. contributed equally to this work.

[2]To whom correspondence may be addressed. Email: louis.taillefer@usherbrooke.ca.

Published August 15, 2022.

Downloaded from https://www.pnas.org by BIBLIOTHEQUE GENERALE (M) on September 20, 2022 from IP address 132.210.82.109.

We report a thermal Hall conductivity among the largest ever observed in an insulator yet, with $\kappa_{xy} \simeq 1$ W/K · m at $T = 20$ K and $H = 15$ T in Cu_3TeO_6. This is 50 times larger than in the cuprate $Sr_2CuO_2Cl_2$, for example. However, the phonon conductivity κ_{xx} is also 50 times larger in Cu_3TeO_6, due to a better sample quality, resulting in less phonon scattering by defects and impurities. Then, the degree of chirality defined by the ratio $|\kappa_{xy}/\kappa_{xx}|$ is similar (in magnitude and temperature dependence) in these two very different materials with different structures, defects, and impurities. This shows that phonon chirality is a much more general phenomenon than hitherto perceived. Because $|\kappa_{xy}/\kappa_{xx}|$ goes smoothly through T_N, we infer that antiferromagnetic order per se is not required, but we speculate that a coupling of phonons to the spin degrees of freedom may nevertheless play a role.

Results

In Fig. 1*A*, the thermal conductivity κ_{xx}, measured at 0 T and 15 T, is plotted as a function of temperature. The field dependence of κ_{xx} is weak, at most 6% (at $T \simeq 20$ K) and negligible for $T > 30$ K (Fig. 1*A*). Our κ_{xx} data are consistent with prior zero-field data (22), where the authors have argued that although magnons below T_N can, in principle, carry heat, phonons dominate the thermal conductivity of Cu_3TeO_6, which is certainly the case above T_N. $\kappa_{xx}(T)$ shows a peak typical of phonons in insulators, located here at $T \simeq 20$ K (Fig. 1*A*).

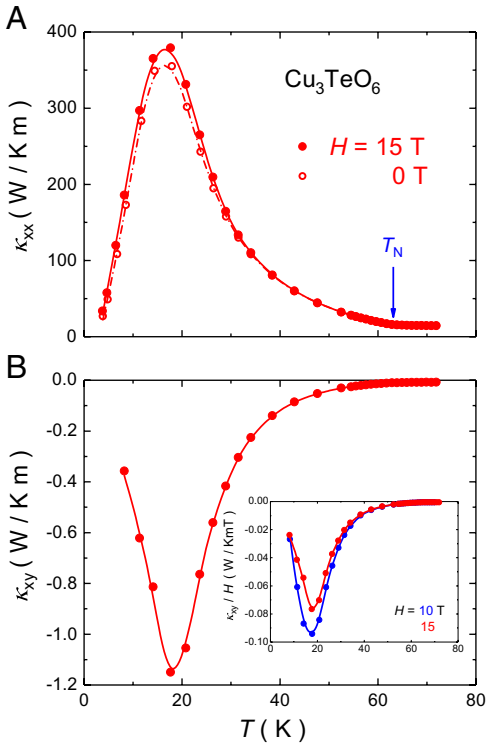

Fig. 1. (*A*) Thermal conductivity κ_{xx} of Cu_3TeO_6 as a function of temperature, in zero field (open circles) and in a magnetic field $H = 15$ T (filled circles). The arrow marks the onset of antiferromagnetic order, at $T_N \simeq 63$ K. (*B*) Corresponding thermal Hall conductivity κ_{xy} at $H = 15$ T. *B*, *Inset* shows the T dependence of thermal Hall conductivity κ_{xy} plotted as κ_{xy}/H at 10 T and 15 T. κ_{xy} scales linearly with H above 40 K. Below 40 K, there is a slight sublinearity. Lines are a guide to the eye. Both $\kappa_{xx}(T)$ and $\kappa_{xy}(T)$ peak at $T \simeq 17$ K, following a large increase relative to their values at T_N, by a factor of ∼25 and ∼150, respectively. The peak value, $|\kappa_{xy}| \simeq 1.0$ W/K · m, is among the largest thermal Hall conductivity reported to date in an insulator.

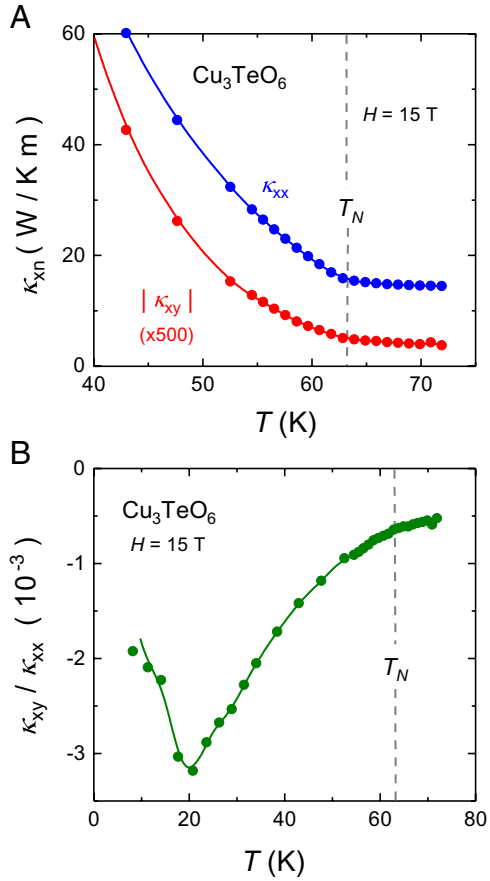

Fig. 2. (*A*) Comparison of $\kappa_{xx}(T)$ (blue) and $\kappa_{xy}(T)$ (red; data multiplied by a factor of 500) near the antiferromagnetic transition at T_N (dashed line). Both curves are seen to rise upon cooling below T_N. (*B*) Ratio of $\kappa_{xy}(T)$ over $\kappa_{xx}(T)$, vs. T, at $H = 15$ T. The magnitude of this ratio increases upon cooling from $T = 70$ K to $T = 20$ K. The fact that it goes smoothly through T_N (dashed line) shows that the onset of long-range magnetic order does not directly affect the thermal Hall effect. Although κ_{xy} in Cu_3TeO_6 is exceptionally large, the maximal value of the ratio, $|\kappa_{xy}/\kappa_{xx}| \simeq 3 \times 10^{-3}$, is typical of various insulators (Table 1). Lines are a guide to the eye.

In Fig. 2*A*, we zoom on the data near T_N. Above T_N, κ_{xx} is flat, evidence that phonons are scattered by spin excitations associated with the proximate onset of antiferromagnetic order (22). Upon cooling below T_N, κ_{xx} suddenly rises, presumably because that scattering is weakened when order sets in.

In Fig. 1*B*, the thermal Hall conductivity κ_{xy}, measured on the same sample in the same conditions, is displayed as a function of temperature. There is a large negative Hall effect. We see that $\kappa_{xy}(T)$ mirrors the evolution of $\kappa_{xx}(T)$, with a peak at the same temperature. As pointed out in ref. 9, this suggests that κ_{xy} is carried predominantly by phonons, as is κ_{xx}. At its peak, $|\kappa_{xy}| \simeq 1.0$ W/K · m, among the largest values of $|\kappa_{xy}|$ reported so far in insulators (Table 1).

In Fig. 2*A*, we see that $\kappa_{xy}(T)$ evolves in tandem with $\kappa_{xx}(T)$ across T_N: It is almost flat above T_N and rises below T_N. This parallel evolution is further evidence that κ_{xy} is carried by phonons. It is instructive to plot the ratio κ_{xy}/κ_{xx} vs. T, as done in Fig. 2*B*, a quantity that may be viewed as the degree of chirality—the extent to which phonons respond asymmetrically to a magnetic field. We see that the ratio goes smoothly through T_N, unaltered by the onset of antiferromagnetic order. This shows that long-range order per se does not play a key role in conferring chirality to phonons. Note that despite the high amplitude of $|\kappa_{xy}|$ in Cu_3TeO_6, the ratio κ_{xy}/κ_{xx} is similar to that found in several other insulators (Table 1), as we discuss below.

Downloaded from https://www.pnas.org by BIBLIOTHEQUE GENERALE (M) on September 20, 2022 from IP address 132.210.82.109.

Table 1. Thermal Hall conductivity in various insulators

Material	κ_{xy}, mW/K · m	κ_{xx}, W/K · m	κ_{xy}/κ_{xx}, 10^{-3}	*T*, *H*; K, T
Cu_3TeO_6	−1,000	330	−3.0	20, 15
$Fe_2Mo_3O_8$ (4)	12	2.5	4.8	65, 14
$Tb_2Ti_2O_7$ (23)	1.2	0.27	4.4	15, 12
$Y_2Ti_2O_7$ (23, 24)	0	18	0	15, 8
La_2CuO_4 (5)	−38	12	−3.2	20, 15
$Sr_2CuO_2Cl_2$ (6)	−21	7	−3.0	20, 15
Nd_2CuO_4 (6)	−200	56	−3.6	20, 15
$SrTiO_3$ (9)	−80	36	−2.2	20, 12
$KTaO_3$ (9)	2	32	0.06	30, 12
$RuCl_3$ (25)	2	2	1.0	20, 15

The values of κ_{xy} and κ_{xx} are taken at the specified temperature *T* and field *H*. Their ratio gives the degree of chirality.

Discussion

In the antiferromagnetic insulator Cu_3TeO_6, two types of neutral excitations can be expected to generate a thermal Hall effect: magnons and phonons. We can rule out magnons, based on our empirical evidence and for theoretical reasons. Empirically, the fact that $\kappa_{xy}(T)$ mirrors the temperature evolution of the phonon-dominated $\kappa_{xx}(T)$ so well (Figs. 1 and 2*A*) argues against a large contribution to κ_{xy} from magnons. Moreover, the fact that the degree of chirality, measured by the ratio κ_{xy}/κ_{xx}, goes through T_N without anomaly (Fig. 2*B*) shows that long-range order, and therefore well-defined magnons, play little role in κ_{xy}. Theoretically, it has been shown that magnons can produce a thermal Hall effect in antiferromagnetic insulators, but only under certain conditions (26). In a collinear antiferromagnet, a condition is the presence of spin canting due to the Dzyaloshinskii–Moriya (DM) interaction. Now in Cu_3TeO_6, theoretical calculations and inelastic neutron scattering experiments show that the collinear antiferromagnetic ground state can be well understood by considering the antiferromagnetic exchange interactions and a global single-ion anisotropy term without introducing any DM interaction (27). Neutron powder diffraction results indicate that the possible noncollinear canting of spins is no more than 6° (20). Under such conditions, the κ_{xy} signal expected from magnons is estimated to be much smaller than the signal reported in La_2CuO_4 (12), which is, in turn, much smaller than what we observe in Cu_3TeO_6. Theory also predicts a sizable thermal Hall effect of magnons in collinear antiferromagnetic insulators with a honeycomb lattice in which there is a spin–flop phase transition (28). However, neither of these features is present in the cubic Cu_3TeO_6 (20). So, the large thermal Hall conductivity in Cu_3TeO_6 is not generated by magnons.

This is in contrast to the case of VI_3, an insulator for which magnons were recently shown to generate a thermal Hall effect (29), because of the large intrinsic DM interaction and associated magnon Berry curvature in that material. The difference between VI_3 and Cu_3TeO_6 shows up clearly in the H dependence of κ_{xy}: κ_{xy} is independent of H in the former and present at $H \simeq 0$, whereas it is roughly linear in H in the latter (Fig. 1 *B*, *Inset*), as in other cases of phonon-mediated thermal Hall effect, including cuprates (6).

We also rule out that κ_{xy} in Cu_3TeO_6 is generated by topological magnons, as is the case in the material VI_3 (29). The topological magnons present in Cu_3TeO_6 are at high energy, namely, 17.75 meV (∼200 K) (27, 30). At $T \sim 20$ K, where κ_{xy} in Cu_3TeO_6 is maximal, these topological magnons are not thermally excited, and the thermal transport is dominated by low-energy acoustic phonons that are not coupled to these topological magnons. These low-energy phonons are coupled to magnons, but nontopological ones at lower energy. So, we conclude that the Dirac magnons in Cu_3TeO_6 do not contribute to the measured thermal Hall effect in this material at low temperature.

The only type of heat carriers left that could generate a thermal Hall effect in Cu_3TeO_6 are phonons. Two empirical observations confirm that it is indeed the phonons that generate the huge κ_{xy} in Cu_3TeO_6. First, $\kappa_{xy}(T)$ and $\kappa_{xx}(T)$ evolve in parallel across the antiferromagnetic transition, both increasing in tandem upon cooling below $T_N \simeq 63$ K (Fig. 2*A*). Second, while the degree of chirality in Cu_3TeO_6 is not exceptionally high, what is exceptionally high among the insulators for which a κ_{xy} signal has been reported is the phonon-dominated κ_{xx} (Table 1). κ_{xy} in Cu_3TeO_6 is very large, simply because κ_{xx} is very large. This is a major finding of this work: The magnitude of κ_{xy} from phonons scales with the magnitude of κ_{xx}. Note also that the field dependence of κ_{xy} in Cu_3TeO_6, displayed in Fig. 1 *B*, *Inset*, is very similar to that of cuprates (6), materials for which the thermal Hall effect is known to arise from phonons (7). So, the record-high thermal Hall conductivity in Cu_3TeO_6 is a property of phonons.

The remaining question is: What makes phonons chiral in Cu_3TeO_6 ? Several authors have proposed that the phonon thermal Hall effect is based on the scattering of phonons by impurities (or defects) (16, 18, 19). This may well be part of the answer. In support of an impurity-based mechanism, we note that $|\kappa_{xy}(T)|$ is maximal at the temperature where κ_{xx} (T) peaks (Fig. 1)—namely, at 20 K, the temperature where impurities (or defects) are expected to be the dominant scattering process. Moreover, the degree of chirality—the ratio $|\kappa_{xy}/\kappa_{xx}|$—is maximal at that temperature (Fig. 2*B*). Note that boundary scattering is the dominant scattering process at the lowest T, with the phonon mean free path (31) approaching the size of our sample at $T \to 0$. However, the mean free path is much shorter at 20 K, by a factor ∼20, due to other scattering processes. The obvious process is scattering by local defects, since the phonons that dominate the thermal conductivity have an energy $\sim 4\ k_B T$ and, thus, a wavelength of ∼4 Å at 20 K—the size of a local defect.

However, within such a class of scenarios, a number of puzzles remain. First, it is clear that not all impurities can generate a phonon thermal Hall effect. For example, there is a κ_{xy} signal in $Tb_2Ti_2O_7$, but not in the closely related material $Y_2Ti_2O_7$ (32). Here, the mechanism is perhaps the presence of Tb ions as superstoichometric impurities that act as skew scatterers, as argued for $Tb_3Gd_5O_{12}$ (3). The question then is: What type of impurity (or defect) can give rise to phonon chirality?

It may be that one should consider not just the impurity, but, rather, the effect of that impurity (or defect) on its local environment. For example, there is a phonon κ_{xy} signal in the cuprate Nd-LSCO at a doping $p = 0.20$, but not in the same material at $p = 0.24$ (5, 7). There is no significant difference between the two dopings in terms of impurities or defects. But the two dopings correspond to different states of matter: the pseudogap phase in the former $(p < p^\star)$ and the strange metal phase in the latter $(p > p^\star)$. So here, it appears that it is the nature of the environment that matters, not the nature of the impurity or defect.

A second puzzle is the fact that the ratio $|\kappa_{xy}/\kappa_{xx}|$ has a similar magnitude (at the peak temperature) in a wide variety of materials with very different types and levels of impurities and defects—namely, $|\kappa_{xy}/\kappa_{xx}| = 3 - 5 \times 10^{-3}$ (at $H = 15$ T) (Table 1). In this respect, it is interesting to compare Cu_3TeO_6

Downloaded from https://www.pnas.org by BIBLIOTHEQUE GENERALE (M) on September 20, 2022 from IP address 132.210.82.109.

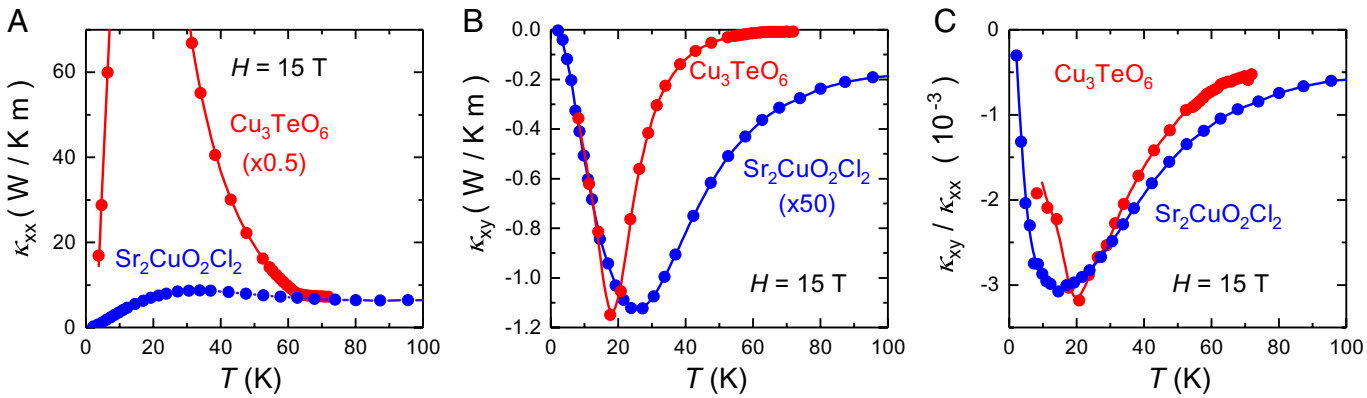

Fig. 3. Comparison of two antiferromagnetic insulators, whose thermal transport was measured in a magnetic field $H = 15$ T: Cu_3TeO_6 (red; this work) and the cuprate Mott insulator $Sr_2CuO_2Cl_2$ [blue (6)]. (*A*) κ_{xx} vs. *T*; the data for Cu_3TeO_6 are multiplied by a factor of 0.5. (*B*) κ_{xy} vs. *T*; the data for $Sr_2CuO_2Cl_2$ are multiplied by a factor of 50. (*C*) κ_{xy}/κ_{xx} vs. *T*; no multiplicative factor. All lines are a guide to the eye.

with $Sr_2CuO_2Cl_2$, as done in Fig. 3. In Fig. 3*C*, we see that the ratio κ_{xy}/κ_{xx} has the same sign, magnitude, and temperature dependence in these two very different materials, even though the level of impurity or defect scattering in the two samples is clearly very different. Indeed, the peak value of κ_{xx} is 50 times larger in Cu_3TeO_6.

A third puzzle arises from this comparison. If the phonon thermal Hall effect is caused by impurity scattering, how can the ratio κ_{xy}/κ_{xx} remain the same in the two materials at all temperatures (Fig. 3*C*), given that in one case (Cu_3TeO_6), the dominant phonon-scattering process goes from impurities at $T = 20$ K to spin fluctuations (and other phonons) at $T = 70$ K, whereas in the other case ($Sr_2CuO_2Cl_2$), it remains impurities at $T = 70$ K? This difference shows up in the T dependence of κ_{xx} (Fig. 3*A*)—nearly constant in $Sr_2CuO_2Cl_2$ and dropping by a factor 20 to 25 in Cu_3TeO_6.

All these suggest that the nature of the environment in which impurities are embedded and phonons propagate matters. We suggest that a magnetic environment—namely, the presence of spins (but not long-range order)—may be relevant. Several authors have shown theoretically that a phonon thermal Hall effect can arise from a coupling of phonons to spins (11, 33–37).

Summary and Outlook

We have measured the thermal conductivity κ_{xx} and the thermal Hall conductivity κ_{xy} of the antiferromagnetic insulator Cu_3TeO_6. We report a value of $|\kappa_{xy}|$ that is among the largest ever observed in an insulator. We provide arguments for why κ_{xy} must be due to phonons, and not magnons. Arguments in favor of phonons include: 1) κ_{xy} (T) and κ_{xx} (T) peak at the same temperature; 2) κ_{xy} and κ_{xx} evolve in the same way across the antiferromagnetic (AFM) ordering temperature T_N; and 3) κ_{xy} scales in magnitude with the phonon-dominated κ_{xx} across various materials, including Cu_3TeO_6. Arguments against magnons include: 1) a magnon Hall effect is ruled out for a collinear AFM order (26); 2) topological magnons are at very high energy (27) and thus irrelevant to the low-energy thermal transport; and 3) a sizable κ_{xy} is observed above T_N, where there are no magnons.

On the basis of a comparison with the cuprate material $Sr_2CuO_2Cl_2$, which exhibits the same ratio κ_{xy}/κ_{xx}, or degree of chirality, both in magnitude and in temperature dependence, even though its phonon conductivity is 50 times smaller, we conclude that the mechanism for phonon chirality could involve the scattering of phonons by impurities or defects. But this scattering process would depend on the nature of the environment in which the impurities or defects are embedded. Although the nature of this coupling remains unclear, we propose that a likely possibility is scattering from local spin texture created by an impurity or defect embedded in a magnetic environment, not necessarily with long-range order. Our findings suggest that a large phonon thermal Hall effect may be a common occurrence in magnetic insulators.

Our findings put two prior studies of the thermal Hall effect into perspective. First, they raise the question of whether the κ_{xy} signal measured in the Kitaev material α-$RuCl_3$ (38), hitherto attributed entirely to Majorana fermions (39), may in part be due to phonons (25). In particular, our finding that the magnitude of κ_{xy} scales with the magnitude of κ_{xx} nicely explains why κ_{xy} in α-$RuCl_3$ varies so much from sample to sample (25, 39–42)—a natural variation in a phonon scenario, where phonon conduction varies due to the sample quality. Secondly, our findings raise the possibility that the phonon thermal Hall conductivity in hole-doped cuprates that appears upon entering the pseudogap phase (5, 7) may be the signature of short-range antiferromagnetic correlations. Data on electron-doped cuprates are consistent with short-range antiferromagnetic correlations playing a role in inducing κ_{xy} (8).

Materials and Methods

Single crystals of Cu_3TeO_6 were grown from CuO powder and TeO_2 flux. The starting materials were mixed in a molar ratio of 3:5 and heated to 870 °C at 5 °C/min, held for 24 h, cooled to 700 °C at 1.5 °C/h, and cooled to room temperature at 3 °C/min. Crystals of approximate dimensions $4 \times 4 \times 1$ mm^3 were harvested after washing the solvent with sodium hydroxide and deionized water. Our sample was cut and polished in the shape of a rectangular platelet, with the following dimensions (length between contacts × width × thickness): $(2.2 \pm 0.1) \times (1.61 \pm 0.04) \times (0.07 \pm 0.01)$ mm. Cu_3TeO_6 has a centrosymmetric cubic crystal structure (20). It is not known to undergo any structural transition. The normal to each of the three faces of the sample is along each of the three equivalent high-symmetry (100) directions of the cubic lattice. Contacts were made by using silver wires and silver paint. The thermal conductivity κ_{xx} and thermal Hall conductivity κ_{xy} were measured as described in refs 5, 6, and 43, by applying a heat current along the *x* axis (longest sample dimension) and a magnetic field along the *z* axis (normal to the largest face) and measuring the longitudinal (ΔT_x) and transverse (ΔT_y) temperature differences with type-E thermocouples.

Data, Materials, and Software Availability. All study data are included in the article.

Downloaded from https://www.pnas.org by BIBLIOTHEQUE GENERALE (M) on September 20, 2022 from IP address 132.210.82.109.

ACKNOWLEDGMENTS. We thank L. Balents, B. Fauqué, I. Garate, N.E. Hussey, S.A. Kivelson, S. Sachdev, R. Valenti, and C.M. Varma for fruitful discussions. L.T. acknowledges support from the Canadian Institute for Advanced Research (CIFAR) as a CIFAR Fellow and funding from the Institut Quantique, the Natural Sciences and Engineering Research Council of Canada (PIN:123817), the Fonds de Recherche du Québec–Nature et Technologies, the Canada Foundation for Innovation, and a Canada Research Chair. This research was undertaken thanks in part to funding from the Canada First Research Excellence Fund. This material is based upon work supported by the Air Force Office of Scientific Research under Award Number FA2386-21-1-4059.

1. C. Strohm, G. L. J. A. Rikken, P. Wyder, Phenomenological evidence for the phonon Hall effect. *Phys. Rev. Lett.* **95**, 155901 (2005).
2. A. V. Inyushkin, A. N. Taldenkov, On the phonon Hall effect in a paramagnetic dielectric. *JETP Lett.* **86**, 379–382 (2007).
3. M. Mori, A. Spencer-Smith, O. P. Sushkov, S. Maekawa, Origin of the phonon Hall effect in rare-earth garnets. *Phys. Rev. Lett.* **113**, 265901 (2014).
4. T. Ideue, T. Kurumaji, S. Ishiwata, Y. Tokura, Giant thermal Hall effect in multiferroics. *Nat. Mater.* **16**, 797–802 (2017).
5. G. Grissonnanche *et al.*, Giant thermal Hall conductivity in the pseudogap phase of cuprate superconductors. *Nature* **571**, 376–380 (2019).
6. M. E. Boulanger *et al.*, Thermal Hall conductivity in the cuprate Mott insulators Nd_2CuO_4 and $Sr_2CuO_2Cl_2$. *Nat. Commun.* **11**, 5325 (2020).
7. G. Grissonnanche *et al.*, Chiral phonons in the pseudogap phase of cuprates. *Nat. Phys.* **16**, 1108–1111 (2020).
8. M. E. Boulanger *et al.*, Thermal Hall conductivity of electron-doped cuprates. *Phys. Rev. B* **105**, 115101 (2022).
9. X. Li, B. Fauqué, Z. Zhu, K. Behnia, Phonon thermal Hall effect in strontium titanate. *Phys. Rev. Lett.* **124**, 105901 (2020).
10. J. Y. Chen, S. A. Kivelson, X. Q. Sun, Enhanced thermal Hall effect in nearly ferroelectric insulators. *Phys. Rev. Lett.* **124**, 167601 (2020).
11. M. Ye, L. Savary, L. Balents, Phonon Hall viscosity in magnetic insulators. arXiv [Preprint] (2021). https://arxiv.org/abs/2103.04223 (Accessed 7 March 2021).
12. R. Samajdar, S. Chatterjee, S. Sachdev, M. S. Scheurer, Thermal Hall effect in square-lattice spin liquids: A Schwinger boson mean-field study. *Phys. Rev. B* **99**, 165126 (2019).
13. Y. Zhang, Y. Teng, R. Samajdar, S. Sachdev, M. S. Scheurer, Phonon Hall viscosity from phonon-spinon interactions. *Phys. Rev. B* **104**, 035103 (2021).
14. C. M. Varma, Thermal Hall effect in the pseudogap phase of cuprates. *Phys. Rev. B* **102**, 075113 (2020).
15. L. Mangeolle, L. Balents, L. Savary, Thermal conductivity and theory of inelastic scattering of phonons by collective fluctuations. arXiv [Preprint] (2022). https://arxiv.org/abs/2202.10366 (Accessed 21 February 2022).
16. B. Flebus, A. H. MacDonald, Charged defects and phonon Hall effects in ionic crystals. *Phys. Rev. B* **105**, L220301 (2022).
17. H. Guo, S. Sachdev, Extrinsic phonon thermal Hall transport from Hall viscosity. *Phys. Rev. B* **103**, 205115 (2021).
18. X. Q. Sun, J. Y. Chen, S. A. Kivelson, Large extrinsic phonon thermal Hall effect from resonant scattering. arXiv [Preprint] (2021). https://arxiv.org/abs/2109.12117 (Accessed 24 September 2021).
19. H. Guo, D. G. Joshi, S. Sachdev, Resonant thermal Hall effect of phonons coupled to dynamical defects. arXiv [Preprint] (2022). https://arxiv.org/abs/2201.11681 (Accessed 27 January 2022).
20. M. Herak *et al.*, Novel spin lattice in Cu_3TeO_6: An antiferromagnetic order and domain dynamics. *J. Phys. Condens. Matter* **17**, 7667 (2005).
21. M. Månsson *et al.*, Magnetic order and transitions in the spin-web compound Cu_3TeO_6. *Phys. Procedia* **30**, 142–145 (2012).
22. S. Bao *et al.*, Evidence for magnon-phonon coupling in the topological magnet Cu_3TeO_6. *Phys. Rev. B* **101**, 214419 (2020).
23. M. Hirschberger, J. W. Krizan, R. J. Cava, N. P. Ong, Large thermal Hall conductivity of neutral spin excitations in a frustrated quantum magnet. *Science* **348**, 106–109 (2015).
24. Q. J. Li *et al.*, Phonon-glass-like behavior of magnetic origin in single-crystal $Tb_2Ti_2O_7$. *Phys. Rev. B* **87**, 214408 (2013).
25. E. Lefrançois *et al.*, Evidence of a phonon Hall effect in the Kitaev spin liquid candidate α-$RuCl_3$. *Phys. Rev. X* **12**, 021025 (2022).
26. H. Katsura, N. Nagaosa, P. A. Lee, Theory of the thermal Hall effect in quantum magnets. *Phys. Rev. Lett.* **104**, 066403 (2010).
27. W. Yao *et al.*, Topological spin excitations in a three-dimensional antiferromagnet. *Nat. Phys.* **14**, 1011–1015 (2018).
28. R. R. Neumann, A. Mook, J. Henk, I. Mertig, Thermal Hall effect of magnons in collinear antiferromagnetic insulators: Signatures of magnetic and topological phase transitions. *Phys. Rev. Lett.* **128**, 117201 (2022).
29. H. Zhang *et al.*, Anomalous thermal Hall effect in an insulating van der Waals magnet. *Phys. Rev. Lett.* **127**, 247202 (2021).
30. S. Bao *et al.*, Discovery of coexisting Dirac and triply degenerate magnons in a three-dimensional antiferromagnet. *Nat. Commun.* **9**, 2591 (2018).
31. S. Y. Li *et al.*, Low-temperature phonon thermal conductivity of single-crystalline Nd_2Cuo_4: Effects of sample size and surface roughness. *Phys. Rev. B* **77**, 134501 (2008).
32. Y. Hirokane, Y. Nii, Y. Tomioka, Y. Onose, Phononic thermal Hall effect in diluted terbium oxides. *Phys. Rev. B* **99**, 134419 (2019).
33. L. Sheng, D. N. Sheng, C. S. Ting, Theory of the phonon Hall effect in paramagnetic dielectrics. *Phys. Rev. Lett.* **96**, 155901 (2006).
34. Y. Kagan, L. A. Maksimov, Anomalous Hall effect for the phonon heat conductivity in paramagnetic dielectrics. *Phys. Rev. Lett.* **100**, 145902 (2008).
35. J. S. Wang, L. Zhang, Phonon Hall thermal conductivity from the Green-Kubo formula. *Phys. Rev. B* **80**, 012301 (2009).
36. L. Zhang, J. Ren, J. S. Wang, B. Li, Topological nature of the phonon Hall effect. *Phys. Rev. Lett.* **105**, 225901 (2010).
37. T. Qin, J. Zhou, J. Shi, Berry curvature and the phonon Hall effect. *Phys. Rev. B* **86**, 104305 (2012).
38. Y. Kasahara *et al.*, Unusual thermal Hall effect in a Kitaev spin liquid candidate α-$RuCl_3$. *Phys. Rev. Lett.* **120**, 217205 (2018).
39. Y. Kasahara *et al.*, Majorana quantization and half-integer thermal quantum Hall effect in a Kitaev spin liquid. *Nature* **559**, 227–231 (2018).
40. P. Czajka *et al.*, The planar thermal Hall conductivity in the Kitaev magnet α-$RuCl_3$. arXiv [Preprint] (2022). https://arxiv.org/abs/2201.07873 (Accessed 19 January 2022).
41. R. Hentrich *et al.*, Unusual phonon heat transport in α-$RuCl_3$: Strong spin-phonon scattering and field-induced spin gap. *Phys. Rev. Lett.* **120**, 117204 (2018).
42. J. A. N. Bruin *et al.*, Robustness of the thermal Hall effect close to half-quantization in α-$RuCl_3$. *Nat. Phys.* **18**, 401–405 (2022).
43. G. Grissonnanche *et al.*, Wiedemann-Franz law in the underdoped cuprate superconductor $YBa_2Cu_3O_y$. *Phys. Rev. B* **93**, 064513 (2016).

Downloaded from https://www.pnas.org by BIBLIOTHEQUE GENERALE (M) on September 20, 2022 from IP address 132.210.82.109.